Luminescence properties of Sn-containing microcrystals in CsBr:Sn crystal

Savchyn P.V.[1], Myagkota S.V.[2], Stryganyuk G.B.[3], Demkiv T.M.[1], Datsjuk J.R.[1], Vus R.B.[2], Demkiv L.S.[4] and Voloshinovskii A.S.[1]

[1] Physics Department, Ivan Franko National University of Lviv,
 8 Kyrylo and Mefodiy St., 79005 Lviv, Ukraine, savchynp@gmail.com
[2] Lviv State Agrarian University, 1 V. Velykyi St., 80381 Dublyany, Ukraine
[3] Institute for Materials, SRC "Carat", 202 Stryiska St., 79031 Lviv, Ukraine
[4] Electronics Department, Ivan Franko National University of Lviv,
 50 Dragomanov St., 79005 Lviv, Ukraine

Abstract

Formation of $CsSnBr_3$ microcrystals in CsBr:Sn (1 mol.%) crystals is revealed after the long-term annealing (t = 100 h, T = 200 ^{0}C). Luminescent-kinetic parameters of CsBr:Sn (1 mol.%) crystals are measured using the excitation with synchrotron radiation. The process of energy transfer from the host to the aggregates is discussed.

Keywords: $CsSnBr_3$ microcrystals, luminescence, energy transfer

1. Introduction

Studies for luminescent-kinetic parameters of semiconducting nano- and microcrystals embedded in different insulator matrices represent one of possible ways for searching the materials of different functional use [1]. The appropriate example of those materials is nano- and microcrystals based on mercury-like ions (Pb^{2+}, Sn^{2+}, Bi^{3+} and Sb^{3+}), which are promising for applications as fast scintillators [2] and active media of thin-film solid state lasers [3].

A luminescence in the red and infrared ranges of the optical spectrum and unusually high conductivity as for ionic semiconductors (10^{-3} (ohm cm)$^{-1}$ in the order of magnitude) are typical to single $CsSnBr_3$ crystals. However, any applications of $CsSnBr_3$ crystal are hindered by their hydration and oxidation in air. So embedding of $CsSnBr_3$ microcrystals in the CsBr matrix seems to offer one of the possible solutions for this problem.

The doping of alkali halide crystals with the mercury-like ions leads to creation of uncompensated charges. Therefore the cation vacancies appear in the crystal volume, which compensate the charges. Further on, they form single Sn^{2+}–v_c^- centres with the mercury-like ions, capable of aggregating into micro- or nanophases embedded in the alkali halide host. Investigations of the aggregation processes of single Sn^{2+}–v_c^- centres in

the CsBr:Sn crystals using the X-ray and optical spectroscopic techniques have revealed formation of Cs_4SnBr_6 and $CsSnBr_3$ microcrystals embedded in the CsBr matrix [4]. Cathodoluminescence properties of Cs_4SnBr_6 and $CsSnBr_3$ microcrystals and their bulk analogues have been found to be identical.

Aiming to elucidate the mechanisms for migration and transformation of high-energy electronic excitations in CsBr crystals that contain $CsSnBr_3$ microcrystals, in this work we study the luminescent-kinetic properties of CsBr:Sn crystals at low temperatures (T = 10 K) and in a wide (4–16 eV) energy range, using the excitation with the synchrotron radiation.

2. Experimental

CsBr:Sn crystals (1 mol.% in the melt) were grown with the Bridgman-Stockbarger technique. A long-term (t = 100 h) annealing (T = 200 ^{0}C) of CsBr:Sn crystal was performed subsequently in order to promote thermally activated migration of ions resulted in the formation of $CsSnBr_3$ microphase embedded in the CsBr matrix.

Measurements of the emission and luminescence excitation spectra and the decay kinetics were performed under the excitation with synchrotron radiation from DORIS storage ring (DESY, Hamburg), using the facility of SUPERLUMI station at HASYLAB [6]. A cryostat with flowing helium was used to carry out low-temperature (T = 10 K) measurements. The emission spectra were studied within the range of 300–1100 nm with the spectral resolution of 1 nm, using Action Research Corporation (ARC) "Spectra Pro 308" 30 cm monochromator-spectrograph equipped with the Princeton Instruments CCD detector and HAMAMATSU R6358P photomultiplier (PMT). The excitation spectra were scanned with the resolution of 3.2 Å within 3.7–15 eV by means of primary 2 m monochromator in 15° McPearson mounting and ARC monochromator as a secondary one. The luminescence decay kinetics was studied in the range of 200 ns using time-correlated single-photon counting technique.

3. Experimental results and discussion

The luminescence spectra of CsBr:Sn crystals excited in the transparency region (λ_{exc} = 195 nm) and the fundamental absorption region (λ_{exc} = 96 nm) of CsBr matrix are shown in Fig. 1. The maxima of the main emission bands of CsBr:Sn crystal are observed at 350, 485, 605, 730 and 1000 nm.

The spectral position of the band peaked at 350 nm is identical to that of the emission band characteristic of the triplet self-trapped exciton (STE) of CsBr matrix [7]. Efficient excitation of this luminescence band in the regions of excitonic and band-to-band absorption of CsBr matrix confirms that this emission may be really attributed to the triplet STE of CsBr matrix (see Fig. 2a).

The luminescence band with the maximum at 485 nm is efficiently excited on the long-wave side of the fundamental absorption region of CsBr matrix. The structure of the
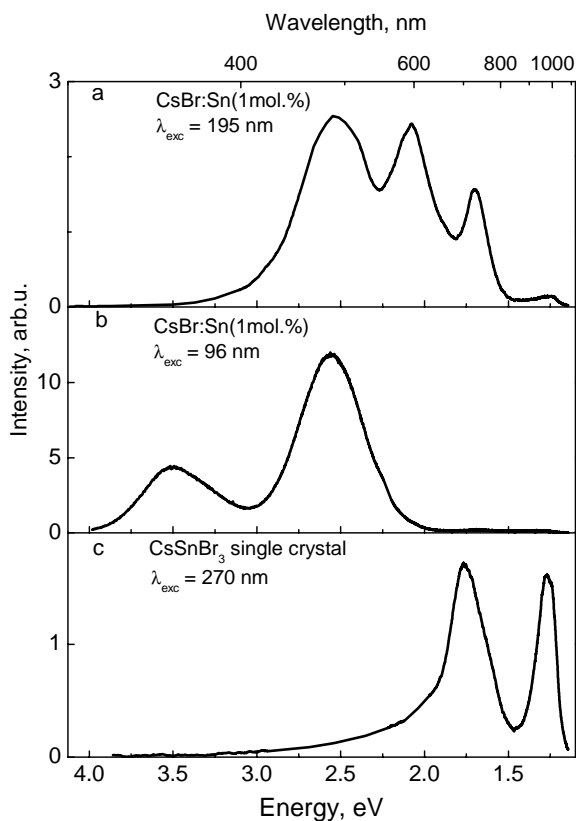
Fig. 1. Emission spectra for CsBr:Sn (1 mol.%) crystal at λ_{exc} = 195 nm (a), λ_{exc} = 96 nm (b) and for CsSnBr$_3$ single crystal at λ_{exc} = 270 nm (c) measured at T = 10 K.

excitation spectrum of this luminescence at the band-to-band transitions in CsBr matrix is similar to the excitation spectrum of the STE emission (see Fig. 2b and 2a, respectively). Such a structure of the excitation spectrum in the region of generation of electron-hole pairs is typical for the excitation spectrum of near-activator exciton luminescence. For example, a similar structure of the excitation spectrum has been detected for the near-activator exciton in CsBr:Tl crystal [8].

The excitation spectrum of the luminescence band peaked at 605 nm reveals a structure characteristic for the emission of single mercury-like centres and contains the bands with the maxima located near 300, 275 and 245 nm 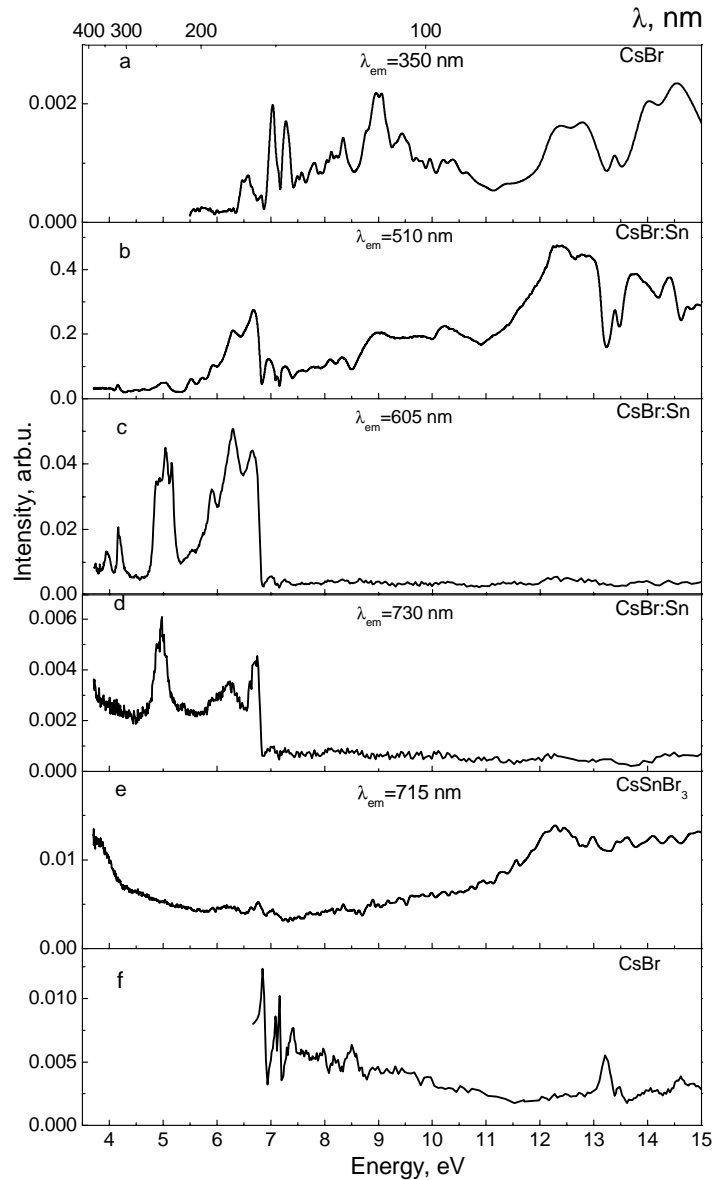(see Fig. 2c). This fact has allowed us to compare these bands with the intra-centric transitions in Sn^{2+} ion [9] and indicate them as A, B and C bands, respectively. As a result, the band peaked at 605 nm can be ascribed to the luminescence of single Sn^{2+}–v_c^- centres in the CsBr matrix.

Concerning their spectral positions, the luminescence bands with the maxima at 730 and 1000 nm are similar to the intrinsic luminescence bands of single CsSnBr$_3$ crystal located at 705 and 980 nm, respectively (Fig. 1c). According to the works [10, 11], the luminescence band peaked at 730 nm can be ascribed to the STE emission of CsSnBr$_3$. Then the band around 1000 nm corresponds to the radiative transition of electron from the 5s5p Sn^{2+} state at the bottom of the conduction band to the conduction sub-band placed lower and created by the 4d states of Br$^-$ ion .

Similarity of the luminescent characteristics of CsBr:Sn and CsSnBr$_3$ in the 700–1000 nm spectral region points out to the formation of CsSnBr$_3$ phase in CsBr:Sn crystal, thus confirming our earlier conclusion about the formation of microphase based upon cathodoluminescence and scanning electron microscopy data [4]. The microphotographs of freshly cleaved surface of CsBr:Sn (1 mol.%) obtained with the scanning electron microscopy reveals that the average radius of the aggregates is $R \approx 5$ µm (see Fig. 3).

Fig. 2. Excitation spectra for CsBr crystal at $\lambda_{em} = 350$ nm (a), CsBr:Sn (1 mol.%) crystal at $\lambda_{em} = 510$ nm (b), 605 nm (c) and 730 nm (d), CsSnBr$_3$ crystal at $\lambda_{em} = 715$ nm (e), and reflection spectrum for CsBr crystal (f). The temperature is T = 10 K.

In order to estimate a possibility of quantum confinement effect in CsSnBr$_3$ aggregates, we suggest the following considerations. Basing on the STE character of the emission and the ionic type of the chemical bond in CsSnBr$_3$ crystal, one can state that the excitonic radius R_{ex} of CsSnBr$_3$ crystal does not exceed half the crystal lattice constant for the cubic modification of the structure ($a = 5.804$ Å) [13]. In other words, we have $R_{ex} < 2.9$ Å, since the exciton is localized at Sn^{2+} ion [10]. According to the study [12], the quantum confinement effect is not observed if the average radius of microcrystal

is $R > 10R_{ex}$. Therefore, the R parameter should not exceed 29 Å in order that the quantum confinement effect could appear. The radius of the CsSnBr$_3$ phase (50×10^3 Å) is significantly greater than the radius of the microcrystal needed to observe the quantum confinement effect. The data associated with the luminescence spectra confirm this conclusion because the characteristic blue shift of the luminescence bands in the 700–1000 nm region of CsSnBr$_3$ microcrystals relatively to ones of CsSnBr$_3$ single crystal is not observed.
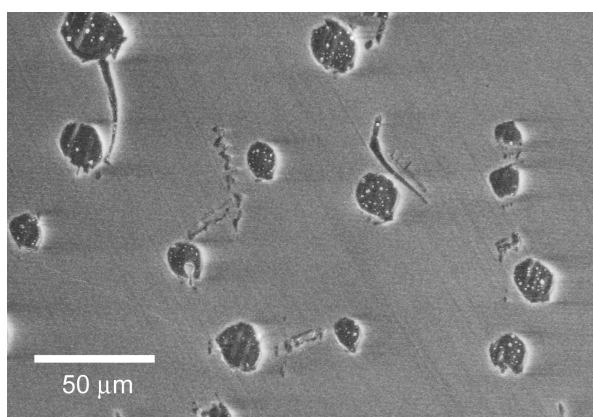

Fig. 3. Microphotographs of freshly cleaved surface of CsBr:Sn (1 mol.%) crystal.

At the same time, a long-wave shift of these bands can be clearly seen (see Fig. 1a and Fig. 1c). The factor that could cause this shift is hydrostatic pressure that affects the microcrystals in the CsBr matrix. Since Sn^{2+} and Pb^{2+} ions are isoelectronic, we suppose that the mechanisms for formation of CsSnBr$_3$ microcrystals and isostructural CsPbBr$_3$ nanocrystals in the CsBr matrix are analogous [14]. Then the ribs of the elementary cell of CsSnBr$_3$ crystal along a and b directions are parallel to the elementary cell diagonals of CsBr (see Fig. 4). The crystal lattice parameter of CsBr is equal to $a = 4.29$ Å [15] and, as mentioned above, the same parameter for the cubic structure of CsSnBr$_3$ is $a = 5.804$ Å. Thus, one can state that the crystal lattice parameters along the a and b directions are expanded up to 6.07 Å, whereas the parameter along the c direction is compressed down to 4.29 Å. These structural changes can indeed result in a long-wave shift of the maximum of STE emission band for the CsSnBr$_3$ microcrystal. Besides, the CsSnBr$_3$ microcrystals are also under influence of the CsBr matrix, due to a difference between the thermal expansion coefficients of CsBr host and CsSnBr$_3$ microcrystals.

From the analysis of structure of the excitation spectra for micro- and single CsSnBr$_3$ crystals (see Fig. 2c, d and e, respectively) it follows that the luminescence of microcrystals is efficiently excited when the energy of the exciting quanta lies in the transparency region of CsBr matrix ($E < 6.7$ eV). The boundary between the transparency and absorption regions of the CsBr matrix is clearly seen from the position of the reflection peak of free exciton in the reflectance spectrum of CsBr (see Fig. 2f).
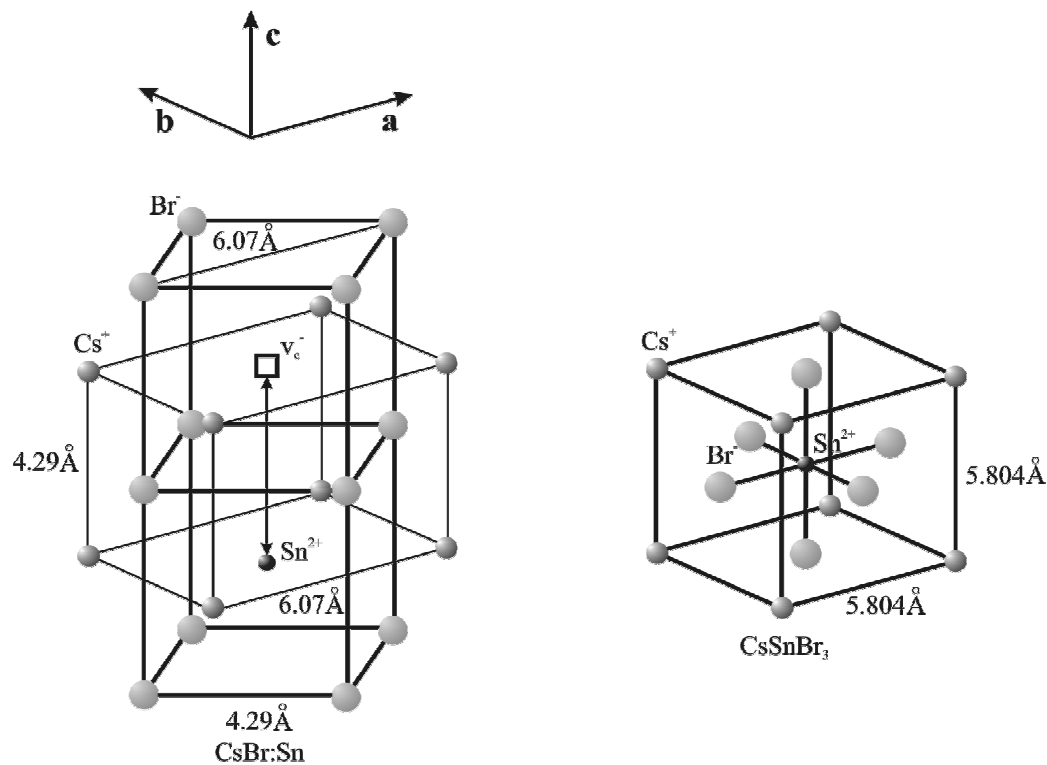
Fig. 4. Schematic representation of crystal lattice structure for CsBr:Sn and CsSnBr$_3$ crystals.

The structure of the excitation spectrum of the emission band peaked at 730 nm for CsSnBr$_3$ microcrystals is similar to the structure typical for mercury-like single Sn^{2+}–v$_c^-$ centres and near-activator excitons in the transparency region of CsBr matrix. This points to the fact that the luminescence of single Sn^{2+}–v$_c^-$ centres and near-activator excitons is reabsorbed by CsSnBr$_3$ microcrystals.

The excitation of CsBr:Sn crystals in the spectral region of absorption of single Sn^{2+}–v$_c^-$ centres and near-activator excitons leads to domination of 'slow' components in the decay kinetics of the emission band with the maximum at 715 nm, due to efficient re-absorption of their luminescence by CsSnBr$_3$ microcrystals. In the case of microcrystals, the decay kinetics curve is characterized with the decay time constants $\tau_f = 5.4$ ns for the 'fast' component and $\tau_s = 1.5$ μs for the 'slow' one, while for the single crystal these constants are $\tau_f = 3.4$ ns and $\tau_s = 0.43$ μs, respectively.

The luminescence excitation efficiency for CsSnBr$_3$ microcrystals in the case of excitation of CsBr:Sn crystal in the region of band-to-band transitions is significantly lower than that typical for the case of excitation in the matrix transparency region. This implies that the relaxed electrons and holes do not participate in the energy transfer from the host to microcrystals.

4. Conclusion

Let us finally summarize in brief the major results derived in the present study:

the long-term annealing (t = 100 h, T = 200 ^{0}C) of CsBr:Sn (1 mol.%) crystals leads to aggregation of Sn^{2+}–v_c^- single centres, with the formation of $CsSnBr_3$ microcrystals;

the luminescence excitation in the $CsSnBr_3$ microcrystals occurs as a result of direct excitation by the light quanta and further re-absorption of the luminescence quanta by single Sn^{2+}–v_c^- centres and near-activator excitons. This re-absorption gives rise to domination of the slow decay component in the decay kinetics peculiar for $CsSnBr_3$ microcrystals;

none energy transfer from the matrix to microcrystals is found upon the band-to-band excitation of CsBr:Sn crystal.

References

1. Nikl M, Polak K, Nitsch K, Pazzi G P, Fabeni P and Gurioli M, 1995. Optical properties of the Pb^{2+}-based aggregated phase in a CsCl host crystal: Quantum-confinement effects. Phys. Rev. B **51:** 5192–5199.
2. Myagkota S V, 1999. X-ray luminescence spectra of Pb^{2+} aggregates in CsX (X = Cl, Br, I) crystals. Opt. Spektr. **87:** 290–294.
3. Kondo S, Kakuchi M, Masaki A and Saito T J, 2003. Strongly Enhanced Free-Exciton Luminescence in Microcrystalline $CsPbBr_3$ Films. J. Phys. Soc. Jap. **72:** 1789–1791.
4. Savchyn P V, Myagkota S V, Voloshinovskii A S, Demkiv T M and Datsjuk J R, 2007. Luminescent properties of Sn-based microcrystals embedded in CsBr matrix. Rad. Meas. **42:** 697–700.
5. Voloshinovskii A, Myagkota S, Demkiv T, Datsjuk J and Demkiv L. Luminescent material. Declaration patent of Ukraine on the useful model. MPK G01T1/28, No u 2007 01472, approved 12.06.2007. Bulletin No 13.
6. Zimmerer G, 1991. Status report on luminescence investigations with synchrotron radiation at HASYLAB. Nucl. Instr. Meth. Phys. Res. A **308:** 178–186.
7. Williams RT and Song KS, 1990. The self-trapped exciton. J. Phys. Chem. Solids. **51:** 679–716.
8. Voloshinovskii A, Zazubovich S, Stryganyuk G and Pashuk I, 2005. Luminescence of CsBr:Tl crystals under synchrotron excitation. J. Lumin. **111:** 9–15.
9. Jacobs PWM, 1991. Alkali halide crystals containing impurity ions with the ns^2 ground-state electronic configuration. J. Phys. Chem. Solids. **52:** 35–67.
10. Voloshinovskii A S, Mikhailik V B, Myagkota S V and Pidzyrailo M S, 1992. Electronic states and luminescence properties of $CsSnBr_3$ crystal. Opt. Spektr. **72:** 486–488.
11. Clark S, Flint C and Donaldson J, 1981. Luminescence and electrical conductivity of $CsSnBr_3$, and related phases. J. Phys. Chem. **42:** 133–135.

12. Ekimov A I, Efros Al L and Onushenko A A, 1985. Quantum Size Effect in Semiconductor Microcrystals. Solid State Commun. **56:** 921–924.

13. Zheng Jin-Cheng, Huan CHA, Wee A T S and Kuok M H, 1999. Electronic properties of CsSnBr$_3$: studies by experiment and theory. Surf. and Interf. Anal. **28**: 81 – 83.

14. Aceves R, Babin V, Flores MB, Fabeni P, Maaroos A, Nikl M, Nitsch K, Pazzi G P, Salas R P, Sildos I, Zazubovich N and Zazubovich S J, 2001. Spectroscopy of CsPbBr$_3$ quantum dots in CsBr:Pb crystals. J. Lumin. **93:** 27–41.

15. Narai-Sabo I. Inorganic chemistry. Budapest. Acad. Sci. Hungary (1969).